(39) For a theoretical description of the dependences of ENDOR amplitudes on the mw or rf power, see: van der Drift, E.; Danners, A. J.; Smidt, J.; Plato, M.; Möbius, K., submitted for publication.
(40) Lendzian, F. Diplomarbeit, FU, Berlin, 1978.
(41) Biehl, R.; Hass, Ch.; Kurreck, H.; Lubitz, W.; Oestreich, S. *Tetrahedron* **1978**, *34*, 419.
(42) Lubitz, W.; Dinse, K. P.; Möbius, K.; Biehl, R. *Chem. Phys.* **1975**, *8*, 371.

Electron Nuclear Double Resonance Spectra of Stellacyanin, a Blue Copper Protein

James E. Roberts,[1a] Theodore G. Brown,[1a] Brian M. Hoffman,*[1a] and Jack Peisach[1b]

Contribution from the Department of Chemistry, Northwestern University, Evanston, Illinois 60201, and the Department of Pharmacology, Albert Einstein College of Medicine of Yeshiva University, New York, New York 10461. *Received June 18, 1979*

Abstract: The ^{1}H, ^{14}N, and $^{63,65}Cu$ electron nuclear double resonances (ENDOR) of stellacyanin have been measured. This represents the first published observation of copper ENDOR in a protein. In confirmation of the results of Rist et al.,[13] the cupric ion must have a minimum of two nitrogenous ligands. The Cu hyperfine splitting (hfs) tensor and the quadrupole tensor have been determined, the first such complete characterization for a copper protein. The unusual Cu hyperfine tensor can be explained by assuming a flattened tetrahedral geometry, without assumption as to the nature of the coordinated ligands; the observation of large quadrupole couplings also appears to be an effect of geometry. The coordination of Cu in stellacyanin is discussed in terms of these results.

Introduction

The blue copper proteins contain a mononuclear Cu(II) site that has unusual optical and magnetic properties.[2a] The electronic spectrum is characterized by a very intense absorption near 600 nm with a molar extinction coefficient of the order 10^3–10^4, in contrast to the low molar extinctions of ordinary mononuclear copper complexes, ~1–100. Typically, the EPR spectrum is also quite different from that observed for "normal" copper; the g tensor is nonaxial and both A_z^{Cu}, the copper hyperfine splitting (hfs) constant associated with the largest g value, and A_{iso}^{Cu}, the isotropic coupling, show unusually small values.

On the basis of near-infrared and visible absorption and circular dichroism spectroscopy[2b] and pulsed EPR data,[3] a distorted tetrahedral coordination geometry has been proposed for the blue copper site. It has further been suggested, partially from model compound studies,[4,5] that the intense blue color is due to S → Cu charge-transfer transitions[2b,6] and that the unpaired electron is substantially delocalized onto a sulfur ligand, accounting for the low values of A_z^{Cu}.[7]

For two blue copper proteins, plastocyanin[8] and azurin,[9] the proposal regarding structure has been substantiated by single-crystal X-ray diffraction. In both, the copper is coordinated by nitrogens from two histidines and sulfur atoms, one from methionine and the other from cysteine. The CuN_2S_2 chromophore exhibits distorted tetrahedral stereochemistry. It is perhaps tempting to generalize this arrangement to include other blue copper centers. However, not all of the blue proteins contain methionine; stellacyanin is the typical example in which it is absent.[10]

Stellacyanin[10] is a blue copper protein of no known function. It is obtained from the bark of *Rhus vernicifera*, the Japanese Lac tree, has a molecular weight of ~20 000, and contains one copper atom per molecule. The detailed electronic spectra and EPR have been reported.[10,11] Only one of the copper hyperfine couplings can be determined unambiguously from the EPR, and then only at the Q-band (35 GHz).[11] The other two principal values of the hfs tensor have been determined by linewidth analyses, and conflicting values were obtained.[10,11] Pulsed EPR studies have confirmed that histidine is bound to copper;[12] the presence of two nitrogen ligands was indicated by ENDOR experiments,[12] although the discussion in the published report is somewhat sketchy. This study was also limited in frequency range because of the instrument used, and thus copper ENDOR was unobservable.

In order to more completely define the coordination sphere in stellacyanin, we have reinvestigated its ENDOR. The results of Rist et al.[13] are confirmed, and show that copper has at least two nitrogen ligands; if there is a third nitrogenous base, then two of these ligands must be related by an approximate inversion center. The complete copper hyperfine splitting (hfs) tensor has been determined, resolving the discrepancy between the published values; in addition, the quadrupole splitting tensor has been obtained. These measurements, along with others under way in our laboratory, constitute the first observation of ENDOR from copper, and have allowed the first such complete characterization of the magnetic properties of a blue copper center.

Experimental Section

A sample of stellacyanin in 0.01 M potassium phosphate buffer (pH 7.0), with a copper concentration of ~3 mM, was prepared as discussed elsewhere.[10] ENDOR was observed more readily when this sample was diluted 50% with glycerol. ENDOR experiments were performed at temperatures near 5 K using a Helitran LTD3-110 variable temperature system, and below the λ point of liquid helium by immersing the microwave cavity in a bath of superfluid helium. Both Dewar systems and the ENDOR spectrometer employing 100-kHz detection are described elsewhere.[14] Copper ENDOR was observed using a Waveter Model 2001 signal generator as the radiofrequency source. ^{14}N and Cu ENDOR spectra were obtained by monitoring the dispersion component of the EPR signal at 2.0 K, and ^{1}H and Cu ENDOR were observed at both 2 and 5 K while monitoring the absorption EPR signal. The EPR saturation behavior was essentially Lorentzian,[15] although considerable mixing of dispersion and passage components into the absorption signal was observed at most microwave powers (>~ 0.2 μW). ENDOR spectra were obtained under the following conditions: 2-μW (2 K) and 0.2-mW (5 K) microwave power, a 100-kHz field modulation amplitude of 3–4 G, and radiofrequency (rf) field strength of ~1 G in the rotating frame.

0002-7863/80/1502-0825$01.00/0

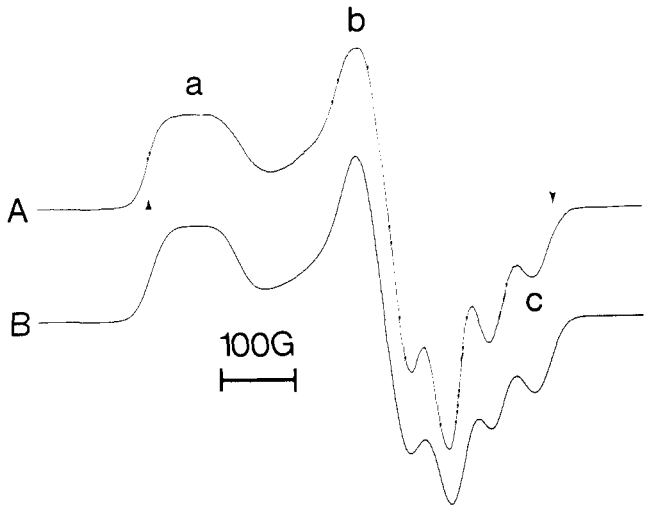

Figure 1. EPR spectrum of stellacyanin. (A) Experimental spectrum; the fields near which ENDOR was done are marked (a) g_z, (b) g_y, and (c) g_x. Microwave frequency, 9210 MHz, T = 77 K. (B) Computer simulation using parameters given in Table I and employing a Gaussian component line of 40 G width. Arrows indicate extremal field positions where ENDOR signals were obtained.

Simulated EPR spectra were calculated using the program SIM 14.[16]

Results

EPR. The 77 K X-band EPR spectrum of stellacyanin is shown in Figure 1. Based on Q-band measurements, the g tensor is reported to be approximately axial with g_x = 2.03, g_y = 2.06, and g_z = 2.30;[11] slightly different values (Table I) are required to best simulate our X-band spectrum (vide infra); however, note that the g values and hyperfine couplings appear to change slightly with medium, making small differences unimportant. The copper hyperfine couplings are only partially resolved and must be considerably smaller than are generally found in monomeric tetragonal copper complexes. Peisach et al.[10] and Malmström et al.[11] have separately estimated the magnitudes of the copper hfs; the estimates do not agree. One conclusion appears firm, however: the largest principal hyperfine coupling does not occur along the same magnetic axis as the maximum g value, as would be expected for a square planar d^9 complex. No ligand hyperfine couplings are observed.

ENDOR Analysis.[13,17-19] The EPR of a frozen solution is a superposition of the resonances from an isotropic distribution of molecular orientations and thus is a summation of signals with the magnetic field H_0 at all possible (θ,ϕ) orientations with respect to the molecular frame. ENDOR is performed by inducing nuclear transitions with a frequency swept rf field, while keeping the external field, H_0, set at a predetermined, fixed value. Therefore, an ENDOR signal arises from that subset of molecules with orientation such that EPR occurs in the vicinity of H_0.[13,18] With H_0 set along z or x (fields marked a and c in Figure 1), "single-crystal like" ENDOR is observed; only copper centers with essentially a single orientation, respectively having H_0 along g_z or g_x, contribute to the ENDOR signal. If the hfs tensor of a nucleus has a principal axis roughly parallel to either axis (x or z), then these ENDOR spectra can be directly interpreted in terms of the principal hfs tensor value.

With the magnetic field set at the derivative feature of the EPR spectrum, labeled b in Figure 1, the observed ENDOR is a superposition from the set of all orientations such that the g factor, $g \equiv g(\theta,\phi)$, obeys the relationship $g^2 = \sum l_i^2 g_i^2 = g_y^2$, where the l_i are the direction cosines of the external field with respect to the ith axis and can be expressed as needed in terms of the Euler angles (θ,ϕ). If we consider a polar coordinate system embedded in a unit sphere on which g is plotted as contours, this set of orientations constitutes a great circle passing tnrough y (θ = 90°, ϕ = 90°) and determined by the above implicit equation $g(\theta,\phi) = g_y$. We note that this treatment neglects the effects of the copper hyperfine coupling on the EPR resonance condition, since at most orientations it is less than, or comparable to, the effective EPR line width (vide infra).

Table I. Spin-Hamiltonian Parameters

axis	z	y	x
stellacyanin			
H (Figure 1)	a	b	c
g value	2.30[a]	2.06[a]	2.03[a]
	2.282[b]	2.075[b]	2.018[b]
$\lvert A^{Cu}\rvert$,[c] MHz	96	87	167[f]
$\lvert P^{Cu}\rvert$,[d] MHz	10	4	6
$\lvert A^{N}\rvert$, MHz	$A_{\parallel}(1) \approx 44$	$A_{\perp}(1) = A_{\perp}(2)$	$A_{\perp}(1) \approx 32$
	$A_{\perp}(2) \approx 32$	≈ 32	$A_{\parallel}(2) \approx 44$
Cu:$Cs_2[ZnCl_4]$[e]			
g value	2.384	2.107	2.083
$\lvert A_i^{Cu}\rvert$, MHz	75	138	153

[a] From ref 10. [b] Values employed in EPR simulation, Figure 1. [c] Best estimate from combined results of ENDOR and of EPR simulations. Estimated, ±5 MHz. [d] Estimated, ±2 MHz. P_y^{Cu} and P_z^{Cu} are of opposite sign from P_x^{Cu}. [e] Reference 23. [f] Limiting value as described in the text.

All ENDOR spectra observed here can be analyzed satisfactorily on the basis of a first-order solution to the electron nuclear spin Hamiltonian. We consider the magnetic field to be along the ith principal axis of the hfs tensor of nucleus, k, with component A_i^k. Then if k is a hydrogen (H), the frequency of the ENDOR signal is given by $\nu_i^H = |\pm A_i^H/2 + \nu_p|$, where ν_p is the free-proton frequency (13.62 MHz at 3200 G). Typically, $A_i^H/2 < \nu_p$ in protein systems, and a pair of lines, symmetrically disposed about ν_p and split by A_i^H, is observed. For ^{14}N, the ENDOR frequencies are $\nu^N = |\pm A_i^N/2 \pm 3P_i^N/2 + \nu_N|$. The ENDOR frequencies depend on both A_i^N and also on P_i^N, the coupling constant for the ith principal axis of the quadrupole tensor. (Note that this expression for ν^N, and that for ν^{Cu} below, employ a traceless quadrupolar Hamiltonian of the form $H_Q = P_1^N(I_1^N)^2 + P_2^N(I_2^N)^2 + P_3^N(I_3^N)^2$.) Since $A_i^N/2$ is typically large compared with P_i^N and ν_N (=0.984 MHz at 3200 G), a single nitrogen will give a four-line pattern centered at $A_i^N/2$.

For a ^{65}Cu or ^{63}Cu nucleus, both with $I = 3/2$, $A_i^{Cu}/2$ is large, and the ENDOR pattern is centered at $A_i^{Cu}/2$. The pattern also includes quadrupole splittings, but in principle contains six lines, not four as for ^{14}N: $\nu^{Cu} = |\pm A_i^{Cu}/2 \pm 3(2m_I^{Cu} - 1)P_i^{Cu}/2 + \nu_{Cu}|$, for nuclear transitions $m_I^{Cu} \rightarrow m_I^{Cu} - 1$, where $m_I^{Cu} = 3/2, 1/2, -1/2$. However, in stellacyanin (and other blue copper proteins) we find that the Cu ENDOR lines are sufficiently broad that splittings by the nuclear Zeeman interaction ($2\nu_{Cu} \approx 7.6$ MHz at 3.2 kG) are unresolvable. In this case the ENDOR pattern should have three features, at frequencies $\nu_{Cu} = |A_i^{Cu}|/2, |A_i^{Cu}|/2 \pm 3|P_i^{Cu}|$.

^{1}H ENDOR. A number of ligand protons with small coupling constants have been seen in the ENDOR of stellacyanin, as well as what appears to be a single proton with a large, nearly isotropic coupling of $|A^H| \approx 20$ MHz.[13] We have confirmed these results, but defer additional discussion of the proton ENDOR until comparisons among several blue copper proteins are possible.

^{14}N ENDOR. In the vicinity of each of the lettered values of H_0 in Figure 1, ENDOR signals were obtained in the 15–26-MHz range, which are assigned to ^{14}N. They are not associated with ^{1}H because they do not shift with changes in the

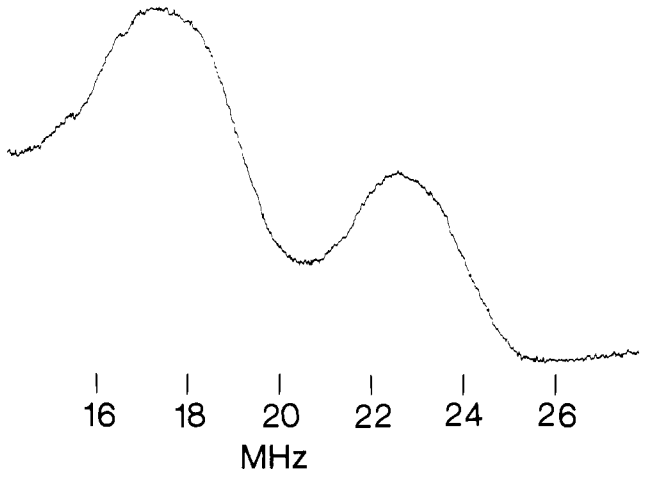

Figure 2. Representative ^{14}N ENDOR spectrum of stellacyanin. H_0 = 2850 G (position a in Figure 1). Absorption intensity centered at ~16 MHz is assigned to N(1); that centered at ~22 MHz to N(2). Microwave frequency, 9210 MHz; $2\nu_N$ = 1.753 MHz; T = 2.0 K.

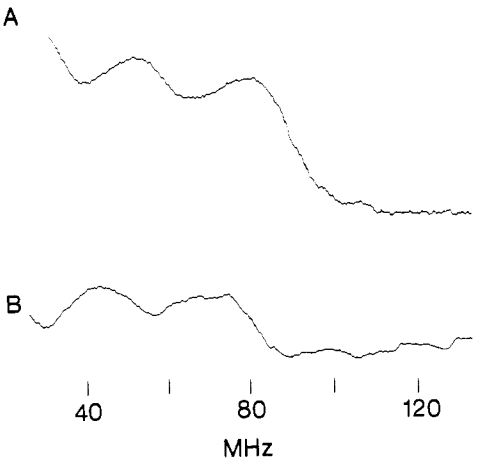

Figure 3. Copper ENDOR of stellacyanin with H_0 = 2800 G, corresponding to field a marked in Figure 1. The pattern does not change for modest changes in field and, for example, is identical at H_0 = 2850 G. Peak positions from spectra taken with increasing (A) and decreasing (B) frequency sweeps are averaged to obtain true values.

microwave frequency, and the copper resonances, described below, are broader and weaker, and primarily occur at higher radiofrequenices. A representative spectrum is shown in Figure 2. Such spectra, first reported by Rist et al.,[13] are quite poorly resolved compared to those which have been seen for ligands of simple "square-planar" copper complexes;[18] one possible reason is a degree of noncollinearity between ^{14}N hyperfine and g tensors. Since our ^{14}N ENDOR spectra are very similar to those originally reported,[13] only the salient features will be mentioned.

At each orientation, ^{14}N absorptions are observed centered at ~16 MHz. Along x(c) and z(a), the absorptions continue to higher frequencies, with a second broad peak at ~22 MHz. A metal-coordinated ^{14}N exhibits a roughly axial hfs tensor, with the unique axis ($\parallel$) corresponding to the M–N bond. These two ENDOR frequencies are, respectively, fairly typical for the perpendicular ($\perp$) and parallel ($\parallel$) hyperfine couplings of a coordinated nitrogen. The observation of absorptions at both 16 and 22 MHz at the same turning point field (Figure 2) therefore requires that two nitrogens be present. We label the nitrogen with the larger hyperfine coupling approximately along the molecular z axis as N(1), and the nitrogen with signal at ~16 MHz along z as N(2). Assuming axial symmetry for the hfs of both nitrogens, we see that the magnitudes of the hyperfine couplings of the two nitrogens are similar, with the axes of the largest couplings approximately at right angles.

Summarizing the ^{14}N data, $A_{\parallel}^{N}(1)$ and $A_{\perp}^{N}(2)$ are observed with H_0 along z, $A_{\perp}^{N}(1)$ and $A_{\parallel}^{N}(2)$ along x, and $A_{\perp}^{N}(1)$ and $A_{\perp}^{N}(2)$ along y (Table I). Based on the pulsed EPR results, at least one of the nitrogens must belong to a coordinated histidine.[12] The similarity of the couplings for N(1) and N(2) suggests that this is true for both, thus supporting a basic parallelism between the site geometry in stellacyanin and that observed by X-ray diffraction of plastocyanin[8] and azurin.[9] While we cannot say for certain that the observed frequencies represent the exact principal couplings of N(1) and N(2), they should be close. In this case, the unique nitrogen hfs tensor axes and thus the Cu–N bonds are aligned approximately along z(N(1)) and x(N(2)) (within ~20°), a result which is also compatible with the pseudotetrahedral geometry found for the blue copper proteins that have been studied by X-ray diffraction.

It is *possible* that more than two nitrogens are coordinated to copper of stellacyanin. Our ENDOR signals would be the same if one of the resonances, say that of N(1), was not from a single ^{14}N, but from a pair of nitrogens related by an approximate center of symmetry. Such could be the case if three nitrogenous ligands and a sulfur ligand are arranged in a flattened tetrahedron of pseudo-D_{2d} symmetry (see below).

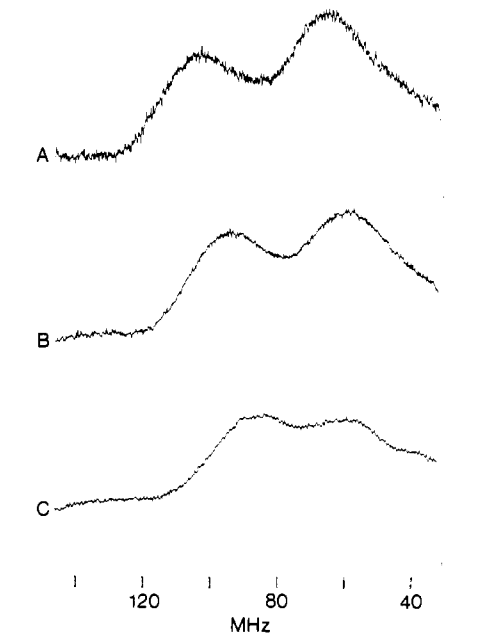

Figure 4. Copper ENDOR of stellacyanin with fields near the position c marked in Figure 1: (A) H_0 = 3350 G (highest field where reasonable signal strength was obtained); (B) H_0 = 3325 G; (C) H_0 = 3300 G. The shifts with field are discussed in the text. The peak positions discussed are again obtained from averaging sweeps of opposite direction (not shown). The copper ENDOR has an opposite phase to the sharp $^{1}H,^{14}N$ peak whose leading edge is seen at the low-frequency edge of the spectrum.

Cu ENDOR. Resonances from copper are clearly observed at frequencies above those for ^{14}N and ^{1}H, although these ENDOR signals are much broader and correspondingly weaker than those for the ligand atoms. Spectra were taken in the vicinity of the lettered fields of Figure 1, as well as at numerous intermediate fields; representative patterns are presented in Figures 3 and 4. The ENDOR signals from copper show a number of interesting characteristics. For example, they depend on the rate with which the radiofrequency field is swept, and they appear as enhanced EPR absorption under some conditions, but as decreased absorption under others. Although we defer any efforts to discuss the spin dynamics associated with these observations, we note that more intense signals are

obtained at sweep rates ($\gtrsim$10 MHz/s) high enough to cause significant shifts of the spectrum. Therefore, results reported here are obtained from averaging peak positions from spectra swept in opposite directions.

As described above, with H_0 along g_z or g_x (near fields a or c), essentially single-crystal-like spectra are expected. The Cu ENDOR pattern obtained from the low-field edge of the EPR spectrum, near a, in insensitive to small change in field and consists of two broad features separated by far more than $2\nu_{Cu}$ (Figure 3). The position of the lower frequency peak corresponds rather well to the value of $|A_z^{Cu}|/2$ predicted from previous EPR spectral simulations.[10,11] We conclude that these two features are those at $|A_z^{Cu}|/2$ and $(|A_z^{Cu}|/2 + 3|P_z^{Cu}|)$, as expected for ENDOR patterns in which the copper nuclear Zeeman splittings are unresolved. The resulting values for $|A_z^{Cu}|$ and $|P_z^{Cu}|$ are given in Table I. The expected third peak, at $(|A_z^{Cu}|/2 - 3|P_z^{Cu}|)$ is calculated to fall under the much more intense $^{14}N,^{1}H$ signals, and presumably is not observed for this reason.

The copper ENDOR spectrum at the highest field edge of the EPR spectrum, near c in Figure 1A, also exhibits two of the three features expected when the nuclear Zeeman splitting is unresolved (Figure 4A). However, spectra taken under a wide variety of conditions, in particular with increasing rf frequency, show that there are only two peaks. Cu ENDOR spectra with two features are also obtained for the largest Cu hfs of azurin from *P. aeruginosa* (unpublished). In azurin, the EPR spectrum shows resolved Cu hfs and we can unambiguously conclude that the two peaks correspond to $(|A_z^{Cu}|/2 \pm 3|P_z^{Cu}|)$; we make the same assignment in stellacyanin.

In a sequence of ENDOR spectra taken at increasingly higher magnetic field values near c, the observed copper ENDOR peaks shift continuously to higher frequency and the observed quadrupolar splitting also increases (Figure 4). Limiting peak positions are clearly being approached in spectra taken at the highest possible field and thus we list in Table I the values of $|A_x^{Cu}|$ and $|P_x^{Cu}|$ so obtained; rigorously, however, by themselves, these should be viewed as constituting lower bounds. Although our experiments give only the $|P_i^{Cu}|$, we can nevertheless assign opposite signs to P_z^{Cu} and P_x^{Cu} through reference to the results of Belford and co-workers.[20] Otherwise, the condition that the quadrupole tensor be traceless would lead to an unreasonably large $|P_y^{Cu}|$.

Fields near b correspond to the third principal g value, g_y, but the EPR signal, and thus the ENDOR signal, at this field consists of contributions from all orientations on the great circle for which $g(\theta,\phi) = g_y$. Examination of the equation for g and for the hyperfine coupling $A = A(\theta,\phi)$, $g^2A^2 = \Sigma g_i^2(A_i^{Cu})^2 l_i^2$, using the measured $|A_z^{Cu}|$, $|A_x^{Cu}|$, and g values (Table I), indicates that $A(\pi/2, \pi/2)/2 = |A_y^{Cu}|/2$ will correspond to the low-frequency extremal value of the ENDOR pattern at b, and that the other extremal value should occur at roughly $A^m/2 \approx A(\pi/3, 0)/2 \approx$ 70–80 MHz. Use of the first-order expression for the angle-dependent quadrupole coupling[19] and the tensor values listed in Table I indicates that quadrupole splittings will be small and unresolved at both extremes of the spectrum. Copper ENDOR spectra taken at b exhibit a broad, unresolved peak extending from a high-frequency end near the predicted value of $A_m/2$ down to ~35 MHz. From the low-frequency end of this pattern, we can do no better than to estimate that $80 \lesssim |A_y^{Cu}| \lesssim 100$ MHz.

The results of the copper ENDOR measurements are in fundamental agreement with the tensor elements (A_z, A_y, A_x) = (105, 87, 171) MHz obtained by Malmström et al. from Q-band EPR spectra and computer simulations,[11] thus qualitatively resolving the discrepancy between previously published sets of copper hfs tensor values. For completeness, it is also of some interest to attempt to assemble our best estimates for the tensor components, recognizing that small differences from those in ref 11 might in some measure reflect influences of the medium, as noted above. An EPR simulation using the hyperfine couplings of Table I gives an excellent fit to the experimental spectrum (Figure 1). Since $|A_x^{Cu}|$ is obtained from ENDOR under the assumption that the center peak in the ENDOR pattern is not seen, this fit supports the assumption, as well as the conclusion, that the limiting hfs splitting in the ENDOR has essentially been achieved.

Discussion

Metal Environment. The copper hyperfine couplings for blue copper proteins such as stellacyanin are quite different from those of the usual tetragonal or distorted square-planar complexes. These latter typically have large and highly anisotropic axial hfs, $A_\parallel^{Cu}$ = 400–600 MHz and $A_\perp^{Cu}$ = 50–100 MHz, with the largest splitting in the same direction as the largest g value.[14,21] The hfs tensor of stellacyanin is also roughly axial, but in contrast the couplings are quite small and the largest hfs is along the minimum g value, as is observed in some tetrahedral or nearly tetrahedral copper complexes.[22,23] These hfs tensor properties are indicative of large p orbital contributions to the d orbital ground state and occur because the p and d orbital contributions to the wave function have anisotropic hfs terms of opposite sign. This orbital mixing is possible in any point group that does not possess a center of symmetry, but for small (D_{2d}) distortions from a square-planar arrangement, the amount of 4p mixing typically is very small. In such systems, the copper hfs remain approximately axial, with a value of $A_\parallel^{Cu}$ only somewhat reduced from the value found in strict D_{4h} symmetry (e.g., Cu(TPP)).[14] The hfs values for stellacyanin thus indicate substantial deviations from D_{4h} symmetry.

In true tetrahedral symmetry, the copper hfs is expected to be nearly isotropic. Two different idealized types of distortion from tetrahedral can be envisioned, both of which lead to hyperfine anisotropy. For a trigonal distortion to molecular C_{3v} symmetry, the odd electron orbital is a mixture of $3d_{z^2}$ and $4p_z$, which is expected to give a large value of A_{iso}^{Cu}.[26] For a D_{2d} distortion, leading to a flattened tetrahedron, the odd electron orbital is a mixture of $3d_{xy}$ and $4p_z$.[23] This geometry is expected to exhibit a reduced A_{iso}^{Cu}, and a minimum hfs component (A_z^{Cu}), which is small and is oriented parallel to the maximum g value. For either type of distortion, the magnetic z axis is predicted to be parallel to the distortion axis. The results for stellacyanin thus are those expected for a flattened tetrahedron (Table I), and the properties of such a geometry are a completely sufficient, and we believe necessary, explanation for the unusual Cu hfs tensor, independent of the nature of the coordinated ligands.

Values of A_i^{Cu} and g_i similar to those of stellacyanin have been observed by Sharnoff[23] for Cu^{2+} ion doped into the flattened tetrahedral Zn site of the $Cs_2[ZnCl_4]$ lattice, as seen in Table I. For this inorganic crystal, the ground-state molecular orbital for the unpaired electron was found to have 70% 3d, 12% 4p, and 18% ligand character. It is important to note that metal ligand covalency without p orbital mixing is not itself sufficient to produce the observed small values of A_i^{Cu}. For example, in Cu(TPP) the unpaired electron wave function has a much lower metal character, but the copper hfs are quite large and anisotropic.[14] In short, the relatively "soft" sulfur ligands(s) may contribute to the stabilization of the essentially tetrahedral structure and produce the typical blue color, but such a ligand is *not* required, per se, to produce the observed magnetic properties of the copper site.

This analysis of the EPR data constitutes an independent confirmation of the conclusions drawn by Gray et al. from optical studies of stellacyanin and other "blue copper" proteins.[2b] The blue color of these proteins is assigned[2b,6] to sulfur-to-metal σ and π charge transfer. The tetrahedral char-

acter of the chromophore leads to additional intense, low-energy d–d transitions.

Our determination of the nuclear quadrupole tensor for the copper provides a new type of information about the type I site, for this coupling reflects an interaction of the copper nucleus with the total nearby electron density, not merely with the odd electron.[20] The tensor is highly rhombic (Table I). This indicates that the pseudoaxial character of the g and hyperfine tensors reflects only an effective symmetry and that the total electron density around the copper deviates appreciably from any idealized symmetry.

The largest quadrupole tensor element for stellacyanin, $P_{max}^{Cu} = |P_x^{Cu}|$, is comparable to that for square-planar $Cu(O)_4$ complexes.[20] At first glance this is surprising. The copper must have at least one S ligand and two N ligands. However, comparing $Cu(S)_4$, $Cu(S_2)(O_2)$, and $Cu(O)_4$ square-planar complexes shows that the covalent character of the Cu–S bond acts to greatly reduce P_{max}^{Cu}.[20] The quadrupole coupling of the copper in stellacyanin probably remains large for reasons related to geometry. First, cancellation of the metal contribution by a contribution from surrounding charges[14] is minimized in a pseudotetrahedral geometry. Second, cancellation through metal–ligand covalency[14] is restricted in a pseudotetrahedral geometry: The "lobes" of the d_{xy} orbital, although drawn out of the plane by mixing with $4p_z$, nonetheless have reduced overlap with the ligand orbitals when compared with a planar complex.[22]

Ligand Arrangement. A final question to be considered is the arrangement of the ligands with respect to the molecular (g-tensor) axes. In all of the published examples of EPR of species with flattened tetrahedral geometry,[26,27,29] the axes of maximum g and minimum A^{Cu} coincide, as observed for the stellacyanin z axis (Table I). However, in the systems of known structure the axis of maximum g corresponds to the distortion axis. If the geometry is indeed D_{2d}, this does not seem to be consistent with the above observation that $A_{\parallel}^{N}(1)$ is roughly along z, since this suggests the ligation of a nitrogen with the M–N bond roughly along the distortion axis. However, in all known systems with similar g values and Cu hfs, the coordination sphere is composed of identical nuclei. It is entirely possible that strong interactions with sulfur orbitals, which are indicated by the low-energy charge-transfer transitions, may rotate the magnetic axes away from the positions indicated by considerations of idealized geometries and idealized distortions.[25] Alternatively, because of the inequivalence of the ligands and, possibly because of additional stereochemical constraints on the copper coordination sphere imposed by the protein in stellacyanin, the distortions of the ideal tetrahedral site may well be neither purely D_{2d} or C_{3v} in nature.

Acknowledgments. This work was supported by the National Institutes of Health (HL-13531), the National Science Foundation (PCM76-81304), and by the NSF–MRL program through the Material Research Center at Northwestern University (DMR 76-80847 A01).

References and Notes

(1) (a) Northwestern University. (b) Albert Einstein College of Medicine of Yeshiva University.
(2) (a) Fee, J. A. *Struct. Bonding (Berlin)* **1975,** *23,* 1–60. (b) Solomon, E. I.; Hare, J. W.; Gray, H. B. *Proc. Natl. Acad. Sci. U.S.A.* **1976,** *73,* 1389–1393. McMillan, D. R.; Holwerda, R. A.; Gray, H. B. *Ibid.* **1974,** *71,* 1339–1341.
(3) Peisach, J.; Mims, W. B. *Eur. J. Biochem.* **1978,** *84,* 207–214.
(4) Thompson, J. S.; Marks, T. J.; Ibers, J. A. *Proc. Natl. Acad. Sci. U.S.A.* **1977,** *74,* 3114–3118.
(5) Jones, M. H.; Levason, W.; McAuliffe, C. A.; Murray, S. G.; Johns, D. M. *Bioinorg. Chem.* **1978,** *8,* 267–278, and references therein.
(6) McMillin, D. R. *Bioinorg. Chem.* **1978,** *8,* 179–184.
(7) Malmström, B. G.; Vänngard, T. J. *J. Mol. Biol.* **1960,** *2,* 118–131.
(8) Colman, P. M.; Freeman, H. C.; Guss, J. M.; Murata, M.; Norris, V. A.; Ramshaw, J. A. M.; Venkatappa, M. P. *Nature (London)* **1978,** *272,* 319–324.
(9) Adman, E. T.; Stenkamp, R. E.; Sieker, L. C.; Jensen, L. H. *J. Mol. Biol.* **1978,** *123,* 35–47.
(10) Peisach, J.; Levine, W. G.; Blumberg, W. E. *J. Biol. Chem.* **1967,** *242,* 2847–2858.
(11) Malmström, B. G.; Reinhammer, B.; Vänngard, T. *Biochim. Biophys. Acta* **1970,** *205,* 48–57.
(12) Mims, W. B.; Peisach, J. *Biochemistry* **1976,** *15,* 3863–3869.
(13) Rist, G. H.; Hyde, J. S.; Vänngard, T. *Proc. Natl. Acad. Sci. U.S.A.* **1970,** *67,* 79–86.
(14) (a) Brown, T. G.; Petersen, J. L.; Lozos, G. P.; Anderson, J. R.; Hoffman, B. M. *Inorg. Chem.* **1977,** *16,* 1563–1565. (b) Brown, T. G.; Hoffman, B. M. *Mol. Phys.*, in press.
(15) Poole, C. P., Jr. "Electron Spin Resonance"; Interscience: New York, 1967.
(16) Lozos, G. P.; Hoffman, B. M.; Franz, C. G. Quantum Chemistry Program Exchange, Indiana University, Bloomington, Ind., Program No. 265.
(17) Kevan, L.; Kispert, L. D. "Electron Spin Double Resonance Spectroscopy"; Wiley: New York, 1976.
(18) Rist, G. H.; Hyde, J. S. *J. Chem. Phys.* **1970,** *52,* 4633–4643.
(19) Abragam, A.; Bleaney, B. "Electron Paramagnetic Resonance of Transition Ions"; Clarendon Press: Oxford, 1970.
(20) White, L. K.; Belford, R. L. *J. Am. Chem. Soc.* **1976,** *98,* 4428–4438; *Chem. Phys. Lett.* **1976,** *37,* 553–557, and references contained therein.
(21) McGarvey, B. R. *J. Phys. Chem.* **1967,** *71,* 51–67.
(22) Bates, C. A.; Moore, W. S.; Standley, K. J.; Stevens, K. W. H. *Proc. Phys. Soc.* **1962,** *79,* 73–83. Bates, C. A. *Ibid.* **1964,** *83,* 465–472.
(23) Sharnoff, M.; Reiman, C. W. *J. Chem. Phys.* **1965,** *43,* 2998–2999. Sharnoff, M. *Ibid.* **1964,** *41,* 2203–2297; **1965,** *42,* 3383–3395.
(24) Goodman, B. A.; Raynor, J. B.; Emeleus, H. S.; Sharpe, A. G. *Adv. Inorg. Chem. Radiochem.* **1970,** *13,* 135–362.
(25) Analogous effects have been observed in nearly square-planar copper complexes for the orientations of the in-plane g tensor axes. See Hitchman, M. A.; Olson, C. D.; Belford, R. L. *J. Chem. Phys.* **1969,** *50,* 1195–1203. Belford, R. L.; Harrowfield, B.; Pilbrow, J. R. *J. Magn. Resonance* **1977,** *28,* 433–439, and references therein.